Data-driven modeling of hysteresis in ReRAM devices: A multifactorial approach for enhanced memory performance

Saba Zamankhani[1]

[1]TU Ilmenau, Department of Computer Science and Automation, Databases and Information Systems Group

Abstract

Many physical systems in the real world exhibit complex behavior, making it difficult to identify their dynamics. To overcome this problem, prototypes are created to provide a better insight into the behavior of such systems. However, building these prototypes using traditional methods is often slow due to the computational intensity required to accurately capture the detailed complexities within these systems and the large parameter space that needs to be explored. Data-driven approaches, such as machine learning and deep learning frameworks, have the potential to significantly speed up this process by generalizing the model. In this study, we explore the use of such an approach to understand the complex and non-linear behavior of dynamical systems, using resistive random access memory (ReRAM) devices as a case study. It is important to emphasize that modeling ReRAM is only one specific example in our wider investigation, which aims to design predictive models for a range of non-linear dynamical systems. Our work attempts to overcome the limitations of traditional research and development by using neural networks to reproduce the complex behavior of ReRAM cells accurately. We introduce a hybrid dual-input neural network architecture (HDiNN), equipped with a custom loss function, to capture both spatial and temporal patterns, improving the predictability of cell behavior under different conditions. This involves integrating important factors such as material properties, device geometry, and electrical interactions into our model to explain the complexities of ReRAM technology. However, our ambitions extend far beyond ReRAM to develop methods to help create innovative, durable solutions in various fields. This study highlights the impact of predictive modeling in advancing materials science and demonstrates the transformative potential of neural networks in improving the design and optimization of future technologies.

Keywords

Non-linear dynamical systems, physical modeling, Resistive random access memory (ReRAM), Hybrid dual-input neural networks

1. Introduction

Many physical systems in the real world, from natural phenomena to engineered materials, show complex behavior. This complexity presents significant challenges, such as the difficulty of predicting system responses under different conditions, the need for extensive computational resources to model these behaviors accurately, and the challenge of translating theoretical models into practical applications. Effective modeling of these systems requires a deep understanding of the behaviors themselves and how they can be replicated and analyzed in a predictive framework[1]. In materials science, for example, this behavior can take many forms, including phase transitions, piezoelectric effects, and memory resistance changes, and represents a fascinating and, at the same time challenging aspect of materials research. However, the journey from concept to the manufacturing of these materials and devices is often costly and time-consuming [2, 3]. To overcome these challenges, researchers are increasingly relying on computational simulations to navigate the complexities of material behavior and device functionality. These simulations allow the exploration of a wide range of parameters and provide insights that guide experimental and design efforts. Although simulations are useful, they can still be time-consuming, which can create a bottleneck in the research and development process. Therefore, it would be beneficial to speed up this process, which can be achieved through the use of data-driven models such as machine learning algorithms. With such models, it is possible to reduce both simulation time and the number of experiments required by accurately predicting the behavior of these complex systems. This would make the research process more efficient and increase the speed with which new materials and devices can be designed. Such predictive capabilities could also serve as a powerful tool for guiding simulation experiments, optimizing resources, and accelerating innovation.

In this work, we will focus on exploring a specific example from materials science: learning the behavior of resistive random access memory (ReRAM) devices. By investigating the dynamic and non-linear behavior associated with these materials, we aim to demonstrate the potential of predictive modeling in advancing the design and optimization of ReRAM technologies and to set a precedent for future research and development in this area.

35th GI-Workshop on Foundations of Databases (Grundlagen von Datenbanken), May 22-24, 2024, Herdecke, Germany.

saba.zamankhani@tu-ilmenau.de (S. Zamankhani)

Table 1
Memrsitive device parameters and their range of values used in the charge transport simulations. [10]

Parameter Name	Symbol	Range	Unit	Parameter type
Band gap	E_{g}	$[0.3, 3.5]$	eV	Material parameters
Electron affinity	χ_{e}	$[1.0, 5.0]$	eV	
Left Schottky barrier	$\phi_0\,(x_1)$	$[0.001, 2]$	eV	
Right Schottky barrier	$\phi_0\,(x_2)$	$[0.001, 2]$	eV	
Relative electric permittivity	ε_{r}	$[1, 15]$	1	
Image-charge rel. el. permittivity	ε_{i}	$[1, 15]$	1	
Electron/hole effective mass	$m_{\mathrm{n}}^*, m_{\mathrm{p}}^*$	$[0.1, 0.9]$	kg	
Electron/hole mobility	$\mu_{\mathrm{n}}, \mu_{\mathrm{p}}$	$[10^{-6}, 500]$	$\mathrm{m}^2/(\mathrm{Vs})$	
Vacancy mobility	μ_{x}	$[10^{-18}, 10^{-8}]$	$\mathrm{m}^2/(\mathrm{Vs})$	Mobile defects
Vacancy energy level	E_{a}	$[0.1, 3.0]$	eV	
Maximum vacancy concentration	N_{x}	10^{28}	m^{-3}	
Channel length	L	$[0.5, 2]$	$\mu\mathrm{m}$	Geometry
Channel width	W	10	$\mu\mathrm{m}$	
Channel thickness	D	0.015	$\mu\mathrm{m}$	
Voltage amplitude	$U_{\max}$	$[5, 13]$	V	Voltage
Voltage period	t_{p}	$[1, 20]$	s	

2. Resistive Random Access Memory (ReRAM)

ReRAM is a class of non-volatile memory that uses the switching properties of materials to enable data storage and retrieval. The switching property refers to the ability of a material within the ReRAM structure to change its electrical resistance between a high resistance state (HRS) and a low resistance state (LRS) in response to an applied voltage [4, 5, 6, 7].

Accurate model of ReRAM is essential for predicting the behaviour of these devices under various conditions, enabling engineers and researchers to simulate and analyse the effects of material properties, device geometry, electrical contacts and applied voltages on device functionality [8, 9] and in general to improve understanding and ability to effectively predicting memristive device behavior.

Many models have been proposed to improve our understanding and ability to effectively predict memristor behavior. These models range from simple representations to complex frameworks that capture the complex dynamics of memristor function [11, 12, 13, 14, 15]. The linear ion drift model is a fundamental approach to the simulation of memristive devices and it is valued for simplicity and ease of use. However, its tendency to oversimplify the complexity of memristor operation and neglect of nonlinear dynamics limits its usefulness for in-depth analysis [11]. At the other end of the complexity spectrum is the Simmons tunnel barrier model, which is notable for its integration of quantum mechanical principles via tunneling effects, providing accurate simulations particularly suited to thin film memristor applications [12]. Meanwhile, models such as the Team model and its Biolek (VTEAM) variant are characterized by their broad coverage and flexibility, being able to model a wide range of memristor behavior by manipulating various parameters [13, 14]. The Generalised Memristor Model takes this flexibility even further by considering a wide range of behaviors and allowing the inclusion of device-specific features [15]. However, the complexity of these models requires significant computational effort and a deep understanding of device parameters to achieve accurate simulations [16, 17].

3. Data-driven Model for ReRAM Behavior Prediction

The use of neural networks accelerates the simulation of ReRAM devices by recognizing relevant features and effectively representing the complex, non-linear dynamics inherent in these devices. Our research aims to predict the behavior of ReRAM devices, considering a range of factors such as material properties, device structure, electrical contacts, and the progression of external voltage over time. An extensive list of discrete parameters incorporated into the model is presented in Table 1.

Recent studies have highlighted the potential of physics-informed neural networks (PINNs) in accurately predicting the behavior of memristive devices and resistive random access memory (ReRAM) [18, 19]. These methods combine traditional physics-based models with neural network techniques to effectively simulate and forecast device behavior. Similarly, Fan et al. [20, 21] introduced graph-based neural networks to capture the intricate details of semiconductor devices, including material properties, device characteristics, and spatial relationships. While promising, these approaches would

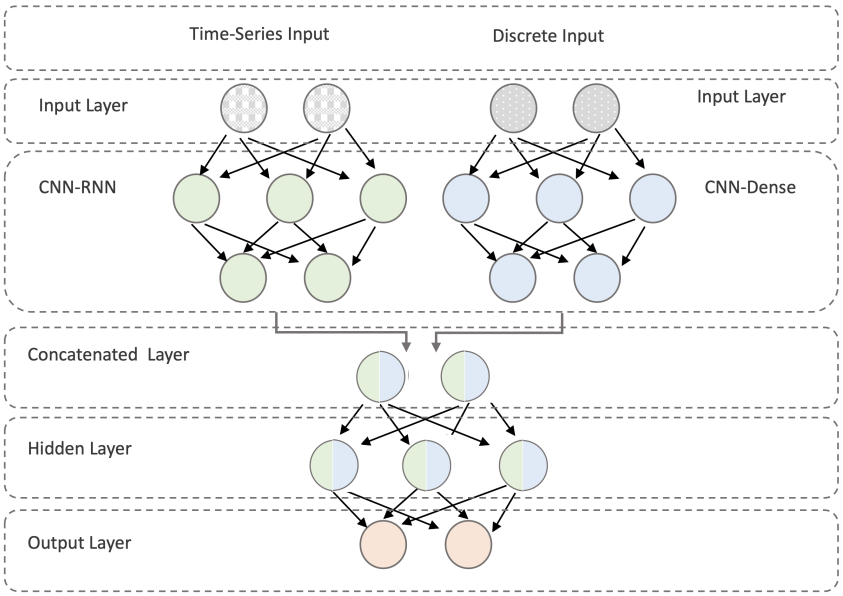

Figure 1: Schematic of the proposed hybrid neural network architecture. The diagram shows the integration of time series and discrete inputs, starting with separate input layers. Time series data is processed through CNN-RNN layers, while discrete inputs pass through a CNN-dense network. Both streams converge in a connected layer, which then feeds into a series of hidden layers for final data storage.

benefit from more extensive experimental validation and comprehensive dataset descriptions to fully demonstrate their effectiveness.

To address these complex challenges, we present a hybrid dual-input neural network (HDiNN) architecture. This framework combines the strengths of convolutional neural networks (CNNs), recurrent neural networks (RNNs), specifically LSTM layers [22], and dense networks [23, 24, 25]. RNNs are used in combination with CNNs to unravel spatial and temporal patterns in sequential data, while CNNs extract features from discrete data points, followed by dense networks to assimilate contextual information [26, 22]. By embedding these extensive parameters into our predictive model, we aim to enhance the understanding of their collective impact on the behavior of ReRAM devices. Our methodology is expected to contribute to the evolution of ReRAM technologies, leading to more efficient, reliable, and scalable memory solutions.

4. Methodology

Our study introduces a dual-input hybrid neural network model to aid the simulation and optimization of ReRAM cells. The basis for the training and validation of our model is a comprehensive dataset derived from a detailed physical charge transport model[10]. The computational model used in this study describes a ReRAM cell based on the presence of mobile charged vacancies in the memristive material. It solves a set of coupled partial differential equations to capture the detailed physical mechanisms that lead to hysteresis in the I-V characteristics of memristive devices. The charge transport model is already validated by measurements [10].

4.1. Hybrid Neural Network Architecture

At the heart of our approach is the development of a hybrid neural network architecture. This architecture uniquely combines the sequential data processing strength of CNNs and RNNs with the skillful parameter handling and feature extraction typical of CNNs followed by dense networks [27, 28, 29, 5]. Figure 1 shows the general schematic of our proposed neural network.

The process starts with a CNN layer, which enhances the feature detection capabilities of the incoming data. This is followed by the RNN segment, which uses LSTM units that are well-suited to recognizing and preserving long-term temporal dependencies. This capability is critical for modeling dynamic systems such as those represented by ReRAM cells. In addition, convolutional layers are embedded within the dense network to detect local spatial features at different scales, enhancing the model's ability to identify intricate patterns in the time

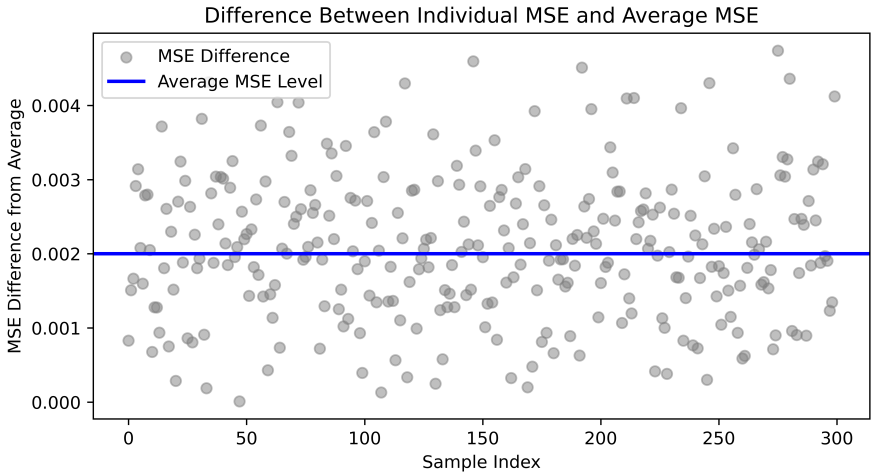

Figure 2: Scatter plot shows the deviation of individual MSE values from the average MSE for a set of test samples. The blue line represents the average level of MSE across all samples, providing a reference for comparing the variance of individual sample errors from this baseline.

series data.

The dense network segment is specifically used to manage discrete parameters, such as material properties and geometric configurations, which are critical in influencing device performance. The outputs from both the CNN-RNN and CNN-dense network segments are merged to create a cohesive representation that encapsulates both temporal dynamics and specific parameter information. This aggregated feature set is then processed through additional dense layers, ultimately leading to an output layer specifically designed to predict the desired current (I) response of a memristive device under varying operating conditions.

4.2. Loss Function

In this work, we introduce a composite loss function, designed to optimize model performance by minimizing prediction error, ensuring trend accuracy, prioritizing critical points, and being robust to outliers. The loss function consists of several components, each addressing different aspects of prediction fidelity. Below, we mathematically describe each component and their integration into the composite loss [30, 31].

Mean Squared Error (MSE): The MSE component quantifies the average of the squares of the errors between the predicted values (y_{pred}) and the actual values (y_{true}). It is defined as:

$$\text{MSE} = \frac{1}{n}\sum_{i=1}^{n}(y_{pred_i} - y_{true_i})^2 \tag{1}$$

Gradient Error: This measures the error in the rate of change between consecutive predictions and actual values, emphasizing the importance of capturing trends. It is computed as:

$$\text{Gradient Error} = \frac{1}{n-1}\sum_{i=1}^{n-1}\left(|y_{pred_{i+1}} - y_{pred_i}| - |y_{true_{i+1}} - y_{true_i}|\right)^2 \tag{2}$$

Peak MSE Loss: This component assigns additional weight to errors at peak points, where the actual data exhibits significant changes. Peaks are identified where the gradient of the actual data exceeds a defined multiple of its maximum value. The Peak MSE loss is defined as:

$$\text{Peak MSE} = \frac{1}{n}\sum_{i=1}^{n} w_{peak}\cdot(y_{pred_i} - y_{true_i})^2 \cdot \text{peak}_i \tag{3}$$

where w_{peak} is the weight assigned to peak points, and $peak_i$ is a binary indicator that equals 1 for data points identified as peaks and 0 otherwise. The formulation ensures that errors at peak points are amplified by the weight w_{peak}.

The final composite loss function integrates the above components with weighting factors to balance their contributions. It is defined as:

$$\text{Combined Loss} = \alpha\cdot\text{MSE} + (1-\alpha)\cdot\text{Gradient Error} + \text{Peak MSE} \tag{4}$$

where α is a weighting factor that balances the contribution of MSE and Gradient Error.

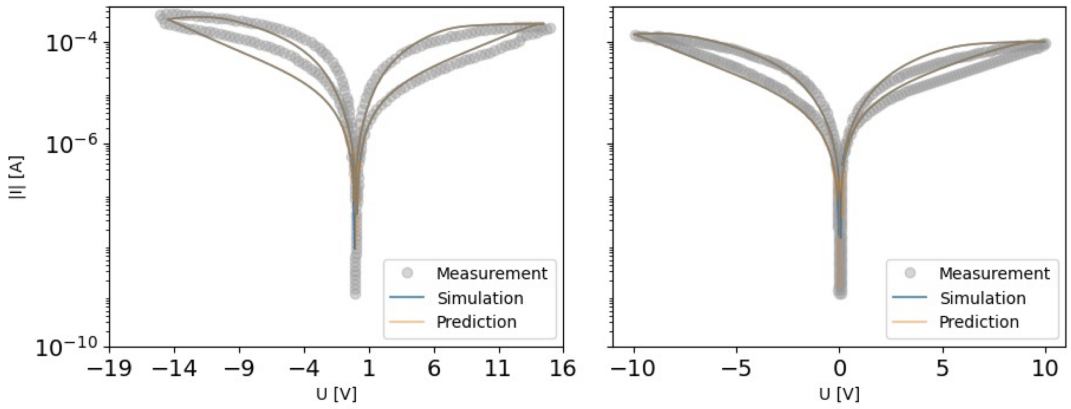

Figure 3: Comparison of experimental data and simulations and our selected approach in two distinct output.

5. Experimental Setup

In this study, we used a dataset comprising 1000 simulations derived from the physical charge transport model as described in Section 4. The dataset includes 16 model parameters as inputs, a sequence of implemented voltages, and the corresponding current as outputs [10]. To generate the dataset, the set of input parameters were systematically varied over a physically reasonable range, as shown in Table 1 [32, 33, 34].

To manage computational demands and optimize processing time, we downsampled the time-series data by randomly selecting 20 % of the samples to retain, removing the remaining samples. This downsampling step ensures the manageability of the dataset without compromising its diversity.

The dataset was divided into a training set (70 % of the total data) and a test set (30 % of the total data). The training set was used to fit the network parameters and generate an accurate forecasting model, while the test set was used to evaluate the performance of the models.

Normalization was applied to all input parameters, scaling them to a uniform range between 0 and 1 to facilitate effective training. The model's output was the prediction of resistance based on the given input parameter set and sequence of voltage. Each set of experiments was run five times to account for the stochastic nature of neural network training.

To evaluate the accuracy of our model, we compared its predictions with the dataset generated from the physical charge transport model using standard regression metrics. The mean squared error (MSE), for a dataset of length N is calculated by measuring the average squared differences between predicted values y and ground truth $\hat{y}$. We also use the mean absolute error (MAE), to measure average absolute difference between y and $\hat{y}$.

6. Results and discussion

The hybrid dual-input neural network (HDiNN) developed to estimate the behavior of ReRAM cells gives encouraging results. Models effectiveness is measured by its ability to mimic the current values of ReRAM devices. The current predictions were found to be in close agreement with both simulation results and experimental data.

It is important to note that since our model was trained exclusively on simulation data rather than actual experimental measurements, it does not surpass the accuracy of the simulation data. The main purpose of comparing the experimental data with the models predictions and simulations is to validate the quality of the simulations used in the training process. An additional consideration in our research is the exclusion of real-world measurements, largely because many of the parameters outlined in Table 1 are not easily accessible in experimental observations, whereas they can be precisely controlled and recorded in simulations.

Another reason for using a data-driven hybrid neural network approach is computational time efficiency. While a single simulation run can take approximately 4 hours, the total training time for the neural network is typically less than 1 hour. This significant difference in time efficiency highlights the advantage of using our HDiNN model, especially in scenarios where rapid iteration and model refinement are critical.

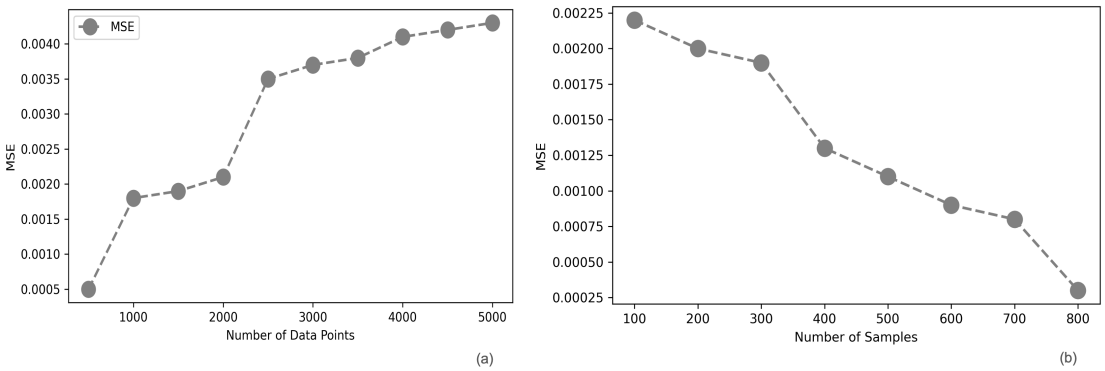

Figure 4: (a) an analysis of prediction lengths versus MSE shows a slight increase in MSE with extended prediction spans; (b) the plot shows a positive correlation between dataset size and prediction accuracy, suggesting improved performance with increasing volume of training data.

In quantitative terms, HDiNN designed to predict the current behavior in ReRAM cells registered MSE of 0.002 and MAE of 0.0029. For a more comprehensive understanding of the prediction quality, we evaluated the variance of the MSE for each prediction relative to the average MSE, as shown in Figure 2. Furthermore, to qualitatively show the accuracy of the model, we examined two different case studies where the model predictions, the simulated data, and the actual measured data are compared, as shown in Figure 3. We evaluated the performance of our model over different prediction lengths and dataset sizes (Figure 4.a,b). Despite a slight increase in MSE with longer prediction spans, the models maintained consistent accuracy, indicating their robustness to different simulation scales(Figure 4.a). Furthermore, our results revealed a positive correlation between the size of the training dataset and prediction accuracy, highlighting the importance of comprehensive training data in the development of robust memristor models (Figure 4.b).

7. Future Work

The results of the model presented are promising, but there are several areas for future research to improve the potential of ReRAM. Despite progress, ReRAM technologies still face challenges such as inconsistent resistance conditions, limited read/write longevity, and the search for a standardized switching mechanism. Overcoming these obstacles is essential to meet the demanding reliability standards needed to bring this revolutionary data storage technology to the mass market.

For future work, our research aims to extend the applicability of our data-driven models beyond the domain of resistive random access memory devices to a broader range of nonlinear dynamical systems in various disciplines. We will explore the potential of neural networks to uncover the complexity of these systems.

Funding

The research is funded by the Carl-Zeiss Foundation via the Project Memwerk, the Deutsche Forschungsgemeinschaft (DFG, German Research Foundation)– Project-ID 434434223 – SFB 1461.

References

[1] P. G. Drazin, Nonlinear systems, 10, Cambridge University Press, 1992.

[2] B. Fultz, Phase Transitions in Materials, 2 ed., Cambridge University Press, 2020.

[3] L. Chua, Memristor-the missing circuit element, IEEE Transactions on circuit theory 18 (1971) 507–519.

[4] M.-K. Song, J.-H. Kang, X. Zhang, W. Ji, A. Ascoli, I. Messaris, A. S. Demirkol, B. Dong, S. Aggarwal, W. Wan, S.-M. Hong, S. G. Cardwell, I. Boybat, J.-s. Seo, J.-S. Lee, M. Lanza, H. Yeon, M. Onen, J. Li, B. Yildiz, J. A. Del Alamo, S. Kim, S. Choi, G. Milano, C. Ricciardi, L. Alff, Y. Chai, Z. Wang, H. Bhaskaran, M. C. Hersam, D. Strukov, H.-S. P. Wong, I. Valov, B. Gao, H. Wu, R. Tetzlaff, A. Sebastian, W. Lu, L. Chua, J. J. Yang, J. Kim, Recent advances and future prospects for memristive materials, devices, and systems 17 (2023) 11994–12039. URL: https://pubs.acs.org/doi/10.1021/acsnano.3c03505. doi:10.1021/acsnano.3c03505.

[5] S. Yu, Neuro-inspired computing with emerging nonvolatile memorys, Proceedings of the

IEEE 106 (2018) 260–285. URL: http://ieeexplore.ieee.org/document/8267253/. doi:10.1109/JPROC.2018.2790840.

[6] S.-J. Li, B.-Y. Dong, B. Wang, Y. Li, H.-J. Sun, Y.-H. He, N. Xu, X.-S. Miao, Alleviating conductance nonlinearity via pulse shape designs in taox memristive synapses, IEEE Transactions on Electron Devices 66 (2019) 810–813. doi:10.1109/TED.2018.2876065.

[7] T.-C. Chang, K.-C. Chang, T.-M. Tsai, T.-J. Chu, S. M. Sze, Resistance random access memory, Materials Today 19 (2016) 254–264. doi:https://doi.org/10.1016/j.mattod.2015.11.009.

[8] R. Dittmann, S. Menzel, R. Waser, Nanoionic memristive phenomena in metal oxides: the valence change mechanism 70 (2021) 155–349. URL: https://www.tandfonline.com/doi/full/10.1080/00018732.2022.2084006. doi:10.1080/00018732.2022.2084006.

[9] M. A. Zidan, J. P. Strachan, W. D. Lu, The future of electronics based on memristive systems, Nature Electronics 1 (2018) 22–29. URL: https://www.nature.com/articles/s41928-017-0006-8. doi:10.1038/s41928-017-0006-8.

[10] B. Spetzler, D. Abdel, F. Schwierz, M. Ziegler, P. Farrell, The role of vacancy dynamics in two-dimensional memristive devices, Advanced Electronic Materials (2023) 2300635. URL: https://onlinelibrary.wiley.com/doi/10.1002/aelm.202300635. doi:10.1002/aelm.202300635.

[11] D. B. Strukov, J. L. Borghetti, R. S. Williams, Coupled ionic and electronic transport model of thin-film semiconductor memristive behavior, Small 5 (2009) 1058–1063. URL: https://onlinelibrary.wiley.com/doi/10.1002/smll.200801323. doi:10.1002/smll.200801323.

[12] M. D. Pickett, D. B. Strukov, J. L. Borghetti, J. J. Yang, G. S. Snider, D. R. Stewart, R. S. Williams, Switching dynamics in titanium dioxide memristive devices, Journal of Applied Physics 106 (2009) 074508. doi:10.1063/1.3236506.

[13] S. Kvatinsky, M. Ramadan, E. Friedman, A. Kolodny, Vteam: A general model for voltage-controlled memristors, Circuits and Systems II: Express Briefs, IEEE Transactions on 62 (2015) 786–790. doi:10.1109/TCSII.2015.2433536.

[14] S. Kvatinsky, E. Friedman, A. Kolodny, U. Weiser, Team: Threshold adaptive memristor model, Circuits and Systems I: Regular Papers, IEEE Transactions on 60 (2013) 211–221. doi:10.1109/TCSI.2012.2215714.

[15] J. Sun, L. Yao, X. Zhang, Y. Wang, G. Cui, Generalised mathematical model of memristor, IET Circuits, Devices & Systems 10 (2016) 244–249.

[16] M. A. Zidan, J. P. Strachan, W. D. Lu, The future of electronics based on memristive systems, Nature Electronics 1 (2018) 22–29. URL: https://api.semanticscholar.org/CorpusID:187510377.

[17] C. Li, D. Belkin, Y. Li, P. Yan, M. Hu, N. Ge, H. Jiang, E. Montgomery, P. Lin, Z. Wang, W. Song, J. P. Strachan, M. D. Barnell, Q. Wu, R. S. Williams, J. J. Yang, Q. Xia, Efficient and self-adaptive in-situ learning in multilayer memristor neural networks, Nature Communications 9 (2018). URL: https://api.semanticscholar.org/CorpusID:256640180.

[18] Y. Lee, K. Kim, J. Lee, A compact memristor model based on physics-informed neural networks, Micromachines 15 (2024) 253.

[19] Y. Sha, J. Lan, Y. Li, Q. Chen, A physics-informed recurrent neural network for rram modeling, Electronics 12 (2023). URL: https://www.mdpi.com/2079-9292/12/13/2906. doi:10.3390/electronics12132906.

[20] G. Fan, K. L. Low, Physics-integrated machine learning for efficient design and optimization of a nanoscale carbon nanotube field-effect transistor, ECS Journal of Solid State Science and Technology 12 (2023) 091005. doi:10.1149/2162-8777/acfb38.

[21] G. Fan, L. Shao, K. L. Low, Revolutionizing tcad simulations with universal device encoding and graph attention networks, arXiv (2023). doi:10.48550/ARXIV.2308.11624.

[22] S. Hochreiter, J. Schmidhuber, Long short-term memory, Neural computation 9 (1997) 1735–80. doi:10.1162/neco.1997.9.8.1735.

[23] D. P. Kingma, J. Ba, Adam: A method for stochastic optimization, arXiv preprint arXiv:1412.6980 (2014).

[24] Y. LeCun, et al., Generalization and network design strategies, Connectionism in perspective 19 (1989) 18.

[25] Y. Bengio, Learning deep architectures for ai, Foundations 2 (2009) 1–55. doi:10.1561/2200000006.

[26] K. Cho, B. van Merrienboer, C. Gulcehre, D. Bahdanau, F. Bougares, H. Schwenk, Y. Bengio, Learning phrase representations using rnn encoder-decoder for statistical machine translation (2014). URL: http://arxiv.org/abs/1406.1078, arXiv:1406.1078 [cs, stat].

[27] T. Wang, J. Roychowdhury, Well-posed models of memristive devices (2016).

[28] S. Furber, Large-scale neuromorphic computing systems 13 (2016) 051001. URL: https://iopscience.iop.org/article/10.1088/1741-2560/13/5/051001. doi:10.1088/1741-2560/13/5/051001.

[29] D. Joksas, A. AlMutairi, O. Lee, M. Cubukcu, A. Lombardo, H. Kurebayashi, A. J. Kenyon, A. Mehonic, Memristive, spintronic, and 2d-materials-based devices to improve and

complement computing hardware, Advanced Intelligent Systems 4 (2022) 2200068. URL: https://onlinelibrary.wiley.com/doi/10.1002/aisy.202200068. doi:10.1002/aisy.202200068.

[30] Q. Wang, Y. Ma, K. Zhao, Y. Tian, A comprehensive survey of loss functions in machine learning, Annals of Data Science 9 (2022) 187–212. doi:10.1007/s40745-020-00253-5.

[31] A. B. Owen, A robust hybrid of lasso and ridge regression, 2006. URL: https://api.semanticscholar.org/CorpusID:1617819.

[32] X. Yan, J. H. Qian, V. K. Sangwan, M. C. Hersam, Progress and challenges for memtransistors in neuromorphic circuits and systems, Advanced Materials 34 (2022) 2108025. URL: https://onlinelibrary.wiley.com/doi/10.1002/adma.202108025. doi:10.1002/adma.202108025.

[33] H. Lee, V. K. Sangwan, W. A. G. Rojas, H. Bergeron, H. Y. Jeong, J. Yuan, K. Su, M. C. Hersam, Dual-gated MoS_2 memtransistor crossbar array, Advanced Functional Materials 30 (2020) 2003683. URL: https://onlinelibrary.wiley.com/doi/10.1002/adfm.202003683. doi:10.1002/adfm.202003683.

[34] G. Ding, B. Yang, R. Chen, W. Mo, K. Zhou, Y. Liu, G. Shang, Y. Zhai, S. Han, Y. Zhou, Reconfigurable 2d WSe_2 -based memtransistor for mimicking homosynaptic and heterosynaptic plasticity, Small 17 (2021) 2103175. URL: https://onlinelibrary.wiley.com/doi/10.1002/smll.202103175. doi:10.1002/smll.202103175.